



Butler University
Digital Commons @ Butler University

Undergraduate Honors Thesis Collection

Undergraduate Scholarship

2019

Seven coordinate molybdenum and tungsten complexes containing Tpm and Tpm derivatives and the impact of ligand substitution on NMR chemical shifts

Cole Seager
Butler University

Follow this and additional works at: <https://digitalcommons.butler.edu/ugtheses>

 Part of the [Biochemistry Commons](#), and the [Chemistry Commons](#)

Recommended Citation

Seager, Cole, "Seven coordinate molybdenum and tungsten complexes containing Tpm and Tpm derivatives and the impact of ligand substitution on NMR chemical shifts" (2019). *Undergraduate Honors Thesis Collection*. 470.

<https://digitalcommons.butler.edu/ugtheses/470>

This Thesis is brought to you for free and open access by the Undergraduate Scholarship at Digital Commons @ Butler University. It has been accepted for inclusion in Undergraduate Honors Thesis Collection by an authorized administrator of Digital Commons @ Butler University. For more information, please contact digitalscholarship@butler.edu.

BUTLER UNIVERSITY HONORS PROGRAM

Honors Thesis Certification


Please type all information in this section:

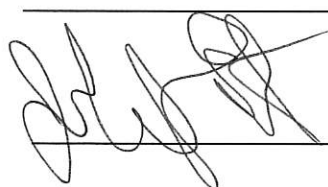
Applicant Cole Brendan Seager
(Name as it is to appear on diploma)

Thesis title Seven coordinate molybdenum and tungsten complexes containing
Tpm and Tpm derivatives and the impact of ligand substitution on
NMR chemical shifts

Intended date of commencement May 11, 2019

Read, approved, and signed by:

Thesis adviser(s)  5/11/2019
Date

Reader(s)  5/11/2019
Date

Date

**Seven coordinate molybdenum and tungsten complexes containing Tpm and Tpm
derivatives and the impact of ligand substitution on NMR chemical shifts**

A Thesis

Presented to the Department of Chemistry and Biochemistry

College of Liberal Arts and Sciences

and

The Honors Program

of

Butler University

In Partial Fulfillment

of the Requirements for Graduation Honors

Cole Seager

May 11, 2019

Seven coordinate molybdenum and tungsten complexes containing Tpm and Tpm derivatives
and the impact of ligand substitution on NMR chemical shifts

Cole Seager and Dr. Stacy O'Reilly

Abstract

A series of known and new seven coordinate molybdenum and tungsten complexes of tris(pyrazolyl)methane (Tpm) and substituted Tpm, $[\text{TpmM}(\text{CO})_3\text{X}]^+$, have been synthesized. Depending on the identity of X, (bromo, iodo, hydrido) and the substitution of the Tpm ligand, substantial chemical shift differences are observed for the hydrogen on the central carbon of the Tpm ligand. Factors impacting the chemical shift of the hydrogen on the central carbon of the Tpm ligand, such as the electron donating ability of the Tpm ligand and the electronegativity of the additional ligand on the metal, will be discussed.

List of Abbreviations

Tpm	Tris(pyrazolyl)methane	214 g/mol
Tpm ⁷	Tris(3,5-dimethylpyrazolyl)methane	298 g/mol
Tpm ^{Ph}	Tris(3-phenylpyrazolyl)methane	439 g/mol
Tpm ^{Me}	Tris(5-methylpyrazolyl)methane	256 g/mol
W(CO) ₆	Tungsten hexacarbonyl	352 g/mol
Mo(CO) ₆	Molybdenum hexacarbonyl	264 g/mol
TpmW(CO) ₃	Tris(pyrazolyl)methyltungstentricarbonyl	482 g/mol
TpmMo(CO) ₃	Tris(pyrazolyl)methylmolybdenumtricarbonyl	394 g/mol
Tpm ⁷ W(CO) ₃	Tris(3,5-dimethylpyrazolyl)methyltungstentricarbonyl	566 g/mol
Tpm ⁷ Mo(CO) ₃	Tris(3,5-dimethylpyrazolyl)methylmolybdenumtricarbonyl	478 g/mol
Tpm ^{Ph} W(CO) ₃	Tris(3-phenylpyrazolyl)methyltungstentricarbonyl	710 g/mol
Tpm ^{Ph} Mo(CO) ₃	Tris(3-phenylpyrazolyl)methylmolybdenumtricarbonyl	622 g/mol
Tpm ^{Me} W(CO) ₃	Tris(5-methylpyrazolyl)methyltungstentricarbonyl	524 g/mol
CO	Carbon monoxide	28 g/mol
FTIR	Fourier-Transform Infrared Spectroscopy	
HNMR	Hydrogen Nuclear Magnetic Resonance	
CNMR	Carbon Nuclear Magnetic Resonance	
DMF	Dimethylformamide	

Introduction

Within many chemistry applications, there can be different molecules that have the ability to covalently bind to a central metal atom. These molecules are known as ligands, and when they bind to metal atoms, they form coordination complexes. These metal coordination complexes are extremely important because they have such versatile use within many realms of chemistry. These metal complexes are widely used as industrial catalysts, and many of these catalysts are growing in interest due to their ability to control chemical reactivity. However, one of their most significant uses is within biochemical applications. Many metal complex enzymes are present within a biological system that utilize a wide variety of metals like iron, zinc, and molybdenum. These complexes can serve a variety of purposes, such as affecting the rate at which carcinogenic cells can be mutated within the body. There are certain chemical functional groups, such as pyrazole (**Figure 1**) and pyrazole-related derivatives, that are known to inhibit several enzymes which commonly have a metal ion as the prosthetic group (the group permanently bound to a protein). Such examples of these enzymes that can be inhibited by pyrazole groups are alcohol dehydrogenases and tryptophan oxygenases.¹

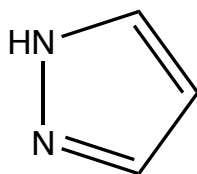


Figure 1: Pyrazole

As ligands, such as carbon monoxide (CO), approach a metal center in an octahedral geometry, the electrons from the ligand interact with the outermost orbitals of the metal. For transition metals, the d orbitals are the frontier orbitals and strongly interact with the incoming

ligands. Some d orbitals, such as the d_{xy} , d_{xz} , and d_{yz} orbitals, do not interact directly with the incoming ligand in a sigma bonding fashion. This discrepancy in the interactions, leading to a loss of degeneracy, is known as d orbital splitting.

Carbon monoxide (CO) ligands have empty antibonding π orbitals. The carbon-oxygen antibonding orbitals can overlap with the metal t_{2g} orbitals, and this overlap allows CO to act as a π -acceptor ligand. If the t_{2g} orbitals are occupied, the metal can move electron density from the metal center to the ligand. This interaction is depicted below with the red arrows. In the case of the CO ligand, the antibonding π orbitals and the t_{2g} orbitals on a metal center are known to have some of the strongest interactions with one another. Shown below is an image of the electrons in the t_{2g} orbital in a metal center interacting with the empty π^* antibonding orbitals of the CO ligand, shown below in **Figure 2**. The sharing of electron density strengthens the bond between the metal center and the carbon atom of the CO ligand, and weakens the C-O triple bond. Since the metal center is acting as a Lewis base, this act of pushing electron density from an electron-rich metal center to π antibonding orbitals of a ligand is known as back bonding.

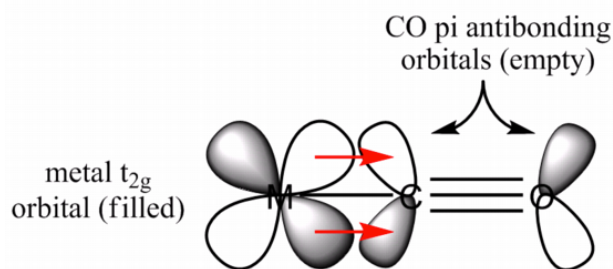


Figure 2: Image of electrons being shared between filled metal t_{2g} orbitals and CO π^* antibonding orbitals

The extent of back bonding can be measured through FTIR spectroscopy by observing the change in stretching frequencies of the CO ligands. CO ligands are useful due to their inherent neutrality, their well-documented stretching frequencies, and their ability to act as excellent π -acceptor ligands. An electron rich metal can utilize its electron density and participate in back bonding with the CO π -acceptor ligands. The electron density of the metal center is pushed into the CO π^* antibonding orbital, which effectively shortens the metal-carbon bond and lengthens the C-O bond.

The energy required to stretch the CO bond is given by Planck's equation, where the energy required is proportional to the frequency of the light energy, or inversely proportional to the wavelength of the light.

$$E = h\nu = \frac{hc}{\lambda}$$

In the equation above, h is planck's constant, ν is the frequency of the light energy, c is the speed of light, and λ is the light's wavelength

The energy of the stretch, though, is most commonly related to the wavenumber of the light, ν , which can be related to the light's wavelength.

$$\nu = \frac{1}{\lambda}$$

The energy of a stretch then will be proportional to its wavenumber. A stretch with a higher wavenumber has a larger stretching energy, and is therefore a stronger bond.

$$E = hc\nu$$

Subsequently, electron density is pushed into the C-O antibonding orbital, and the bond is now weakened and elongated, allowing the C-O bond to stretch more easily. As the bond is able to

stretch more easily, the wavenumber is lowered, which is observable and measurable through FTIR spectroscopy. The ability to track the amount of electron density present on the metal center readily available to be pushed to π -acceptor ligands, and the affects that has on the wavenumber of the CO stretch, can be easily tracked. This is relevant because as the complexes undergo various synthetic manipulations, such as changing the metal center, changing the identity of various ligands, or changing the overall charge on the complex, the change in the total electron density at the metal center can be measured by FTIR.

Tris(pyrazolyl)methane ligands

Originally synthesized by Trofimenko in the 1970's, the tris(pyrazolyl)methane ligands, Tpm (**Figure 3**) are a class of ligands called scorpionate ligands.² The facially coordinating neutral ligands can be varied based on the substituents on the pyrazole rings. The various sites on the pyrazole rings are shown in **Figure 3**. The ligand has a three-fold axis of symmetry and the NMR of the parent ligands contains only three signals: three for the hydrogens of the pyrazole rings and one for the hydrogen on the central sp^3 hybridized carbon. Unusually, this hydrogen is observed at 8.57 ppm in the 1H NMR, incredibly downfield for a hydrogen on an sp^3 hybridized carbon.

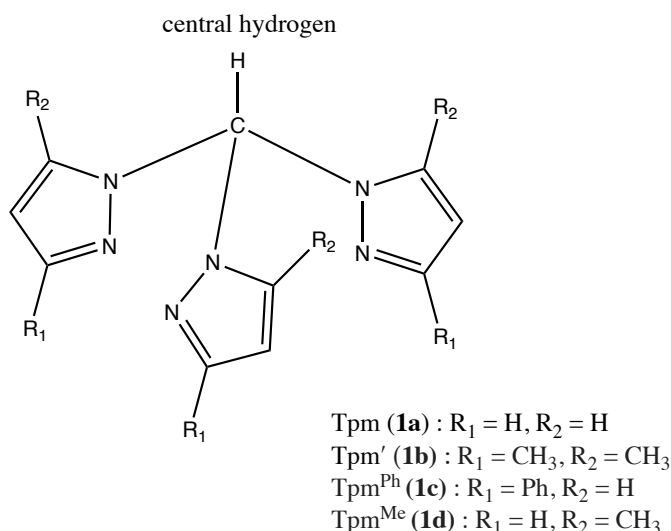


Figure 3: Tris(pyrazolyl)methane ligand (Tpm) and associated derivatives

The structures of these ligands will feature the addition of two methyl groups to the 3,5 positions on the pyrazole rings (**1b**), a phenyl group present on the 3 position of the pyrazole rings (**1c**), and a few examples of a single methyl group in the 5 position of the pyrazole (**1d**). In all cases, the ring maintains its three-fold axis of symmetry. By introducing a variety of newly substituted groups on the original Tpm ligand, the overall electron density present on the metal complex will be altered.

The Tpm ligands can easily be incorporated into Group 6 metal complexes through reaction with hexacarbonyl metal complexes, and many of these reactions were originally reported by Trofimenko.² The six coordinate Tpm tricarbonyl complexes can undergo two electron oxidations by a series of electrophiles. In the oxidized metal complexes, differences in the electron density present within the transition metal complex can not only be measured by changes in the CO stretching wavenumber, but also by changes in the chemical shift of the central hydrogen. An understanding of how electron density travels throughout the transition metal complex can be explored by observing how NMR chemical shifts of the complexes are either heavily affected, or not affected whatsoever.

Experimental Section

All reactions were performed under a nitrogen atmosphere with standard Schlenk techniques. Solvents were using an Mbraun solvent purification system. All reagents were obtained from commercial sources, and used as received, except for tungsten hexacarbonyl which underwent

sublimation. IR spectra were recorded on a Nicolet iS10 FT-IR spectrometer in a methylene chloride solution. ^1H NMR and ^{13}C NMR spectra were recorded on a Bruker 400 Avance MHz NMR, with chemical shifts reported downfield relative to TMS. Tpm^{Mc} was synthesized by Cody Carley, from experimental methods utilized by Goodman et. al.³

Tris(pyrazoly)methane (Tpm, 1a): To a 250 mL round bottom flask was added pyrazole (4.0 g, 59 mmol), tetrabutylammonium bromide (0.95 g, 2.9 mmol) and DI water (60 mL, 3.3 mol). Sodium carbonate (38.2 g, 360 mmol) was gradually added to form a slurry, and chloroform (29 mL, 243 mmol) was added to the slurry. With stirring, the reaction mixture was heated to reflux for four days. After reflux, the solution had separated into a diphasic solution with a suspension of solid Na_2CO_3 . The solid Na_2CO_3 was removed via gravity filtration. Diethyl ether (80 mL) was added, and the aqueous layer was extracted (3 x 40 mL) with diethyl ether. The organic layer was treated with charcoal and magnesium sulfate, which was removed via filtration. The solvent was removed via rotary evaporation to yield 0.36 g (1.7 mmol) of Tpm (**1a**) (57%). ^1H NMR (400 MHz, CDCl_3) δ 8.59 (s, 1H, (pz)₃CH) 7.71 (d, 3H) 7.56 (d, 3H) 6.29 (dd, 3H).

Tris(3,5-dimethylpyrazoly)methane (Tpm', 1b) : To a 250 mL round bottom flask was added 3,5-dimethylpyrazole (6.80 g, 71 mmol), tetrabutylammonium bromide (1.40 g, 4.4 mmol) and DI water (70 mL, 3.8 mol). Sodium carbonate (58.6 g, 552 mmol) was gradually added to form a slurry, and chloroform (30 mL, 260 mmol) was added to the slurry. With stirring, the reaction mixture was heated to reflux for four days. After reflux, the solution had separated into a diphasic solution with a suspension of solid Na_2CO_3 . The solid Na_2CO_3 was removed via gravity

filtration. Diethyl ether (80 mL) was added, and the aqueous layer was extracted (3 x 40 mL) with diethyl ether. The organic layer was treated with charcoal and magnesium sulfate, which was removed via filtration. The solvent was removed via rotary evaporation to yield 0.54 g (1.8 mmol) of **Tpm'** (**1b**) (18%). ¹H NMR (400 MHz, CDCl₃) δ 8.07 (s, 1H, (pz)₃CH) 5.38 (s, 1H, C=CH) 2.19 (s, 1H, C-CH₃) 2.02 (s, 1H, C-CH₃).

TpmW(CO)₃: To a 250 mL three necked flask, W(CO)₆ (1.01 g, 2.87 mmol) and tris(pyrazolyl)methane (0.61 g, 2.8 mmol) in DMF (50 mL) under nitrogen was heated to reflux for approximately 16 hours. The suspension was initially a light yellow-orange in color, and darkened as the reaction proceeded. The mixture was allowed to cool to room temperature and cold methanol (15 mL) was added to the mixture. The mixture was then cooled to 0°, filtered, and the solid was dried under vacuum over night to produce 1.2 g (2.6 mmol) (90%) of a powdery, yellow solid. IR: νCO = 1880, 1743.

TpmMo(CO)₃: To a 250 mL three necked flask, Mo(CO)₆ (1.01 g, 3.84 mmol) and tris(pyrazolyl)methane (0.82 g, 3.8 mmol) in DMF (50 mL) under nitrogen was heated to reflux for approximately 16 hours. The suspension was initially a light yellow-orange in color, and darkened as the reaction proceeded. The mixture was allowed to cool to room temperature and cold methanol (15 mL) was added to the mixture. The mixture was then cooled to 0° C, filtered, and the solid was dried under vacuum overnight to produce 1.4 g, (3.5 mmol) (90%) of a powdery, yellow solid. IR: νCO = 1882, 1763.

Tpm'W(CO)₃: To a 250 mL three necked flask, W(CO)₆ (1.0 g, 2.9 mmol) and tris(3,5-dimethylpyrazolyl)methane (0.82 g, 2.8 mmol) in DMF (50 mL) under nitrogen was heated to reflux for approximately 16 hours. The suspension was initially a light yellow-orange in color, and darkened as the reaction proceeded. The mixture was allowed to cool to room temperature and cold methanol (15 mL) was added to the mixture. The mixture was then cooled to 0° C, filtered, and the solid was dried under vacuum overnight to produce 1.3 g (2.3 mmol) (81%) of a powdery, yellow solid. IR: νCO = 1888, 1750.

Tpm'Mo(CO)₃: To a 250 mL three necked flask, Mo(CO)₆ (1.0 g, 3.8 mmol) and tris(3,5-dimethylpyrazolyl)methane (1.1 g, 3.8 mmol) in DMF (50 mL) under nitrogen was heated to reflux for approximately 16 hours. The suspension was initially a light yellow-orange in color, and darkened as the reaction proceeded. The mixture was allowed to cool to room temperature and cold methanol (15 mL) was added to the mixture. The mixture was then cooled to 0° C, filtered, and the solid was dried under vacuum overnight to produce 1.5 g (3.3 mmol) (85%) of a powdery, yellow solid. IR: νCO = 1900, 1762.

Tpm^{P^h}W(CO)₃: To a 250 mL three necked flask, W(CO)₆ (1.0 g, 2.9 mmol) and tris(3-phenylpyrazolyl)methane (1.3 g, 2.9 mmol) in DMF (50 mL) under nitrogen was heated to reflux for approximately 6 hours. The suspension was initially a light yellow-orange in color, and darkened as the reaction proceeded. The mixture was allowed to cool to room temperature and cold methanol (15 mL) was added to the mixture. The mixture was then cooled to 0° C, filtered, and the solid was dried under vacuum overnight to produce 1.7 g (2.5 mmol) (86%) of a powdery, yellow solid. IR: νCO = 1884, 1749.

Tpm^{Ph}Mo(CO)₃: To a 250 mL three necked flask, Mo(CO)₆ (1.0 g, 3.8 mmol) and tris(3-phenylpyrazolyl)methane (1.7 g, 3.8 mmol) in DMF (50 mL) under nitrogen was heated to reflux for approximately 6 hours. The suspension was initially a light yellow-orange in color, and darkened as the reaction proceeded. The mixture was allowed to cool to room temperature and cold methanol (15 mL) was added to the mixture. The mixture was then cooled to 0° C, filtered, and the solid was dried under vacuum overnight to produce 1.9 g (3.2 mmol) (84%) of a powdery, yellow solid. IR: νCO = 1891, 1759.

Tpm(5-methyl)W(CO)₃: To a 250 mL three necked flask, W(CO)₆ (0.84 g, 2.4 mmol) and tris(5-methylpyrazolyl)methane (0.61 g, 2.4 mmol) in DMF (50 mL) under nitrogen was heated to reflux for approximately 16 hours. The suspension was initially a light yellow-orange in color, and darkened as the reaction proceeded. The mixture was allowed to cool to room temperature and cold methanol (15 mL) was added to the mixture. The mixture was then cooled to 0° C, filtered, and the solid was dried under vacuum overnight to produce 1.0 g (1.9 mmol) (81%) of a powdery, yellow solid. IR: νCO = 1886, 1745.

[TpmW(CO)₃I][I]: To a 50 mL Schlenk flask under nitrogen atmosphere, TpmW(CO)₃ (0.15 g, 0.43 mmol) was dissolved in methylene chloride (15 mL). Elemental iodine (0.11 g, 0.43 mmol) was added, and the solution was stirred for 30 minutes at room temperature. Diethyl ether (15 mL) was added to precipitate a brown-orange solid from solution. The precipitate was collected via cannula filtration and dried under vacuum, yielding 0.19 g (0.31 mmol) (73%). IR: νCO = 2036, 1960, 1928. ¹H NMR (400 MHz, CD₂Cl₂) δ 11.4 (s, 1H, (pz)₃CH) 8.93 (d, Tpm-NCH)

8.50 (d, Tpm-NCH) 6.60 (dd, Tpm-C=CH). ^{13}C NMR (400 MHz, CD_2Cl_2) δ 227.8 (CO) 150.0 (N-N=C), 135.6 (CH-N-C), 109.8 (N-C=C), 73.5 (HC(pz)₃).

[TpmMo(CO)₃I][I]: To a 50 mL Schlenk flask under nitrogen atmosphere, TpmMo(CO)₃ (0.15 g, 0.38 mmol) was dissolved in methylene chloride (15 mL). Elemental iodine (0.10 g, 0.38 mmol) was added, and the solution was stirred for 30 minutes at room temperature. Diethyl ether (15 mL) was added to precipitate a brown-orange solid from solution. The precipitate was collected via cannula filtration and dried under vacuum, yielding 0.15 g (0.29 mmol). (76%) IR: ν_{CO} = 2044, 1976, 1945. ^1H NMR (400 MHz, CD_2Cl_2) δ 11.9 (s, 1H, (pz)₃CH) 9.14 (d, 1H, Tpm-NCH) 8.73 (d, 1H, Tpm-NCH) 6.85 (dd, 1H, Tpm-C=CH). ^{13}C NMR was unattainable due to the fluxional behavior of the Tpm molybdenum complex.

[TpmW(CO)₃H][BF₄]: To a 50 mL Schlenk flask under nitrogen atmosphere, TpmW(CO)₃ (0.15 g, 0.43 mmol) was dissolved in methylene chloride (15 mL). Tetrafluoroboric acid (0.15 mL, 0.78 mmol) in diethyl ether was added, and the solution was stirred for 1 hour at room temperature. Diethyl ether (15 mL) was added to precipitate a white solid from solution. The precipitate was collected via cannula filtration and dried under vacuum, yielding 0.12 g (0.25 mmol) (58%) IR: ν_{CO} = 2022, 1935, 1912. ^1H NMR (400 MHz, CD_2Cl_2) δ 9.56 (s, 1H, (pz)₃CH) 8.38 (d, 1H, Tpm-NCH) 8.15 (d, 1H, Tpm-NCH) 6.47 (dd, 1H, Tpm-CCH) -2.57 (s, 1H, WH) ^{13}C NMR (400 MHz, CD_2Cl_2) δ 215.0 (CO), 149.7 (N-N=C), 135.6 (CH-N-C), 108.3 (N-C=C), 76.5 (HC(pz)₃).

[TpmMo(CO)₃H][BF₄]: To a 50 mL Schlenk flask under nitrogen atmosphere, TpmW(CO)₃ (0.15 g, 0.39 mmol) was dissolved in methylene chloride (15 mL). Tetrafluoroboric acid (0.10 mL, 0.52 mmol) in diethyl ether was added, and the solution was stirred for 1 hour at room temperature. Diethyl ether (15 mL) was added to precipitate a white solid from solution. The precipitate was collected via cannula filtration and dried under vacuum, yielding 0.13 g (0.24 mmol) (60%). IR: $\nu_{\text{CO}} = 2029, 1939, 1921$. ¹H NMR (400 MHz, CD₂Cl₂) δ 9.54 (s, 1H, (pz)₃CH) 8.47 (d, 1H, Tpm-NCH) 8.18 (d, 1H, Tpm-NCH) 6.57 (dd, 1H, Tpm-CCH) -3.08 (s, 1H, MoH). ¹³C NMR was unattainable due to the fluxional behavior of the Tpm molybdenum complex.

[TpmW(CO)₃Br][Br]: To a 50 mL Schlenk flask under nitrogen atmosphere, TpmW(CO)₃ (0.15 g, 0.43 mmol) was dissolved in methylene chloride (15 mL). Bromine solution (0.4 M) in methylene chloride (1.1 mL, 0.43 mmol) was added, and the solution was stirred for 1 hour at room temperature. Diethyl ether (15 mL) was added to precipitate a brown-yellow solid from solution. The precipitate was collected via cannula filtration and dried under vacuum, yielding 0.16 g (0.28 mmol) (66%). IR: $\nu_{\text{CO}} = 2045, 1966, 1925$. ¹H NMR (400 MHz, CD₂Cl₂) δ 13.1 (s, 1H, (pz)₃CH) 8.98 (d, 1H, Tpm-NCH) 8.34 (d, 1H, Tpm-NCH) 6.54 (dd, 1H, Tpm-CCH) ¹³C NMR (400 MHz, CD₂Cl₂) δ 197.2 (CO), 149.4 (N-N=C), 136.6 (CH-N-C), 109.5 (N-C=C), 72.9 (HC(pz)₃).

[TpmMo(CO)₃Br][Br]: To a 50 mL Schlenk flask under nitrogen atmosphere, TpmMo(CO)₃ (0.15 g, 0.39 mmol) was dissolved in methylene chloride (15 mL). Bromine solution (0.4 M) in methylene chloride (0.97 mL, 0.38 mmol) was added, and the solution was stirred for 1 hour at

room temperature. Diethyl ether (15 mL) was added to precipitate a brown-yellow solid from solution. The precipitate was collected via cannula filtration and dried under vacuum, yielding 0.14 g (0.25 mmol) (65%). IR: $\nu_{\text{CO}} = 2056, 1989, 1946$. $^1\text{H NMR}$ (400 MHz, CD_2Cl_2) δ 12.8 (s, 1H, $(\text{pz})_3\text{CH}$) 8.98 (d, 1H, Tpm-NCH) 8.27 (d, 1H, Tpm-NCH) 6.53 (dd, 1H, Tpm-C=CH). $^{13}\text{C NMR}$ was unattainable due to the fluxional behavior of the Tpm molybdenum complex.

[Tpm'W(CO)₃I][I]: To a 50 mL Schlenk flask under nitrogen atmosphere, Tpm'W(CO)₃ (0.15 g, 0.27 mmol) was dissolved in methylene chloride (15 mL). Elemental iodine (0.1 g, 0.3 mmol) was added, and the solution was stirred for 30 minutes at room temperature. Diethyl ether (15 mL) was added to precipitate an orange solid from solution. The precipitate was collected via cannula filtration and dried under vacuum, yielding 0.16 g (0.20 mmol) (74%). IR: $\nu_{\text{CO}} = 2054, 2032, 1931$. $^1\text{H NMR}$ (400 MHz, CD_2Cl_2) δ 7.99 (s, 1H, $(\text{pz})_3\text{CH}$) 6.30 (s, 3H, Tpm-C=CH) 2.73 (s, 9H, C-CH₃) 2.34 (s, 9H, C-CH₃)

[Tpm'Mo(CO)₃I][I]: To a 50 mL Schlenk flask under nitrogen atmosphere, Tpm'Mo(CO)₃ (0.15 g, 0.32 mmol) was dissolved in methylene chloride (15 mL). Elemental iodine (0.1 g, 0.3 mmol) was added, and the solution was stirred for 30 minutes at room temperature. Diethyl ether (15 mL) was added to precipitate an orange solid from solution. The precipitate was collected via cannula filtration and dried under vacuum, yielding 0.13 g (0.18 mmol) (56%). IR: $\nu_{\text{CO}} = 2043, 2019, 1956$. $^1\text{H NMR}$ (400 MHz, CD_2Cl_2) δ 8.14 (s, 1H, $(\text{pz})_3\text{CH}$) 6.36 (s, 3H, Tpm-C=CH) 2.86 (s, 9H, C-CH₃) 2.39 (s, 9H, C-CH₃). $^{13}\text{C NMR}$ was unattainable due to the fluxional behavior of the Tpm' molybdenum complex.

[Tpm'W(CO)₃H][BF₄]: To a 50 mL Schlenk flask under nitrogen atmosphere, Tpm'W(CO)₃ (0.15 g, 0.27 mmol) was dissolved in methylene chloride (15 mL). Tetrafluoroboric acid (0.05 mL, 0.26 mmol) in diethyl ether was added, and the solution was stirred for 1 hour at room temperature. Diethyl ether (15 mL) was added to precipitate a white solid from solution. The precipitate was collected via cannula filtration and dried under vacuum, yielding 0.12 g (0.20 mmol) (78%). IR: ν_{CO} = 2012, 1927, 1893. ¹H NMR (400 MHz, CD₂Cl₂) δ 8.09 (s, 1H, (pz)₃CH) 6.27 (s, 3H, Tpm-CCH) 2.70 (s, 9H, C-CH₃) 2.68 (s, 9H, C-CH₃) -2.45 (s, 1H, WH) ¹³C NMR (400MHz, CD₂Cl₂) δ 212.6 (CO), 156.7 (N-N=C), 145.2 (CH-N-C), 109.3 (N-C=C), 68.9 (HC(pz)₃), 15.1 (H₃C-pz), 12.6 (H₃C-pz).

[Tpm'Mo(CO)₃H][BF₄]: To a 50 mL Schlenk flask under nitrogen atmosphere, Tpm'Mo(CO)₃ (0.15 g, 0.32 mmol) was dissolved in methylene chloride (15 mL). Tetrafluoroboric acid (0.04 mL, 0.26 mmol) in diethyl ether was added, and the solution was stirred for 1 hour at room temperature. Diethyl ether (15 mL) was added to precipitate a white solid from solution. The precipitate was collected via cannula filtration and dried under vacuum, yielding 0.12 g (0.25 mmol) (74%). IR: ν_{CO} = 2020, 1938, 1918. ¹H NMR (400 MHz, CD₂Cl₂) δ 8.03 (s, 1H, (pz)₃CH) 6.23 (s, 3H, Tpm-CCH) 2.68 (s, 9H, C-CH₃) 2.67 (s, 9H, C-CH₃) -3.35 (s, 1H, MoH)

[Tpm'W(CO)₃Br][Br]: To a 50 mL Schlenk flask under nitrogen atmosphere, Tpm'W(CO)₃ (0.15 g, 0.27 mmol) was dissolved in methylene chloride (15 mL). Bromine solution (0.4 M) in methylene chloride (0.78 mL, 0.30 mmol) was added, and the solution was stirred for 1 hour at room temperature. Diethyl ether (15 mL) was added to precipitate a brown-yellow solid from

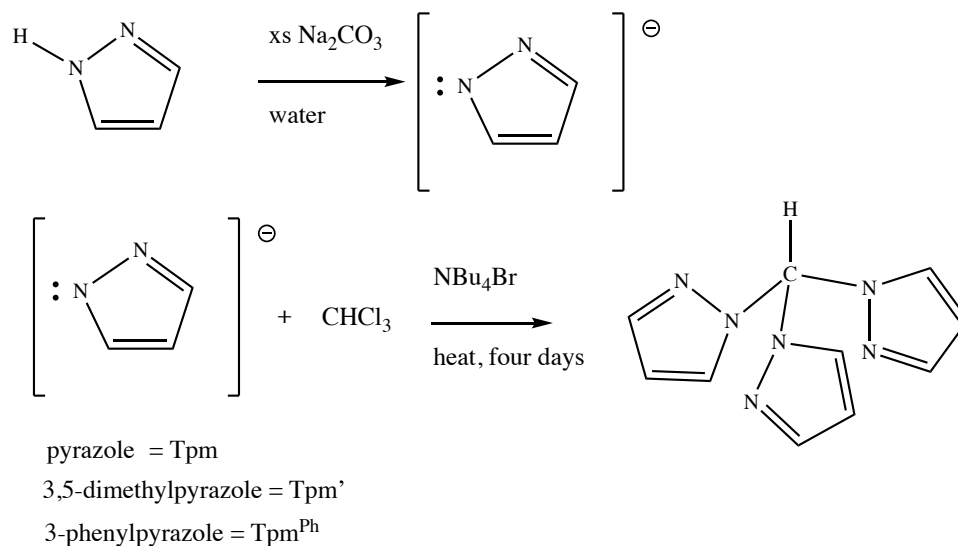
solution. The precipitate was collected via cannula filtration and dried under vacuum, yielding 0.13 g (0.22 mmol) (79%). IR: ν_{CO} = 2036, 1958, 1928. ^1H NMR (400 MHz, CD_2Cl_2) δ 8.03 (s, 1H, $(\text{pz})_3\text{CH}$) 6.29 (s, 3H, Tpm-CCH) 2.75 (s, 9H, C- CH_3) 2.32 (s, 9H, C- CH_3)

[Tpm'Mo(CO)₃Br][Br]: To a 50 mL Schlenk flask under nitrogen atmosphere, Tpm'Mo(CO)₃ (0.15 g, 0.32 mmol) was dissolved in methylene chloride (15 mL). Bromine solution (0.4 M) in methylene chloride (0.81 mL, 0.32 mmol) was added, and the solution was stirred for 1 hour at room temperature. Diethyl ether (15 mL) was added to precipitate a brown-yellow solid from solution. The precipitate was collected via cannula filtration and dried under vacuum, yielding 0.14 g (0.23 mmol) (68%). IR: ν_{CO} = 2048, 1973, 1952. ^1H NMR (400 MHz, CD_2Cl_2) δ 8.16 (s, 1H, $(\text{pz})_3\text{CH}$) 6.23 (s, 3H, Tpm-CCH) 2.80 (s, 9H, C- CH_3) 2.25 (s, 9H, C- CH_3). ^{13}C NMR was unattainable due to the fluxional behavior of the Tpm molybdenum complex.

Results and Discussion

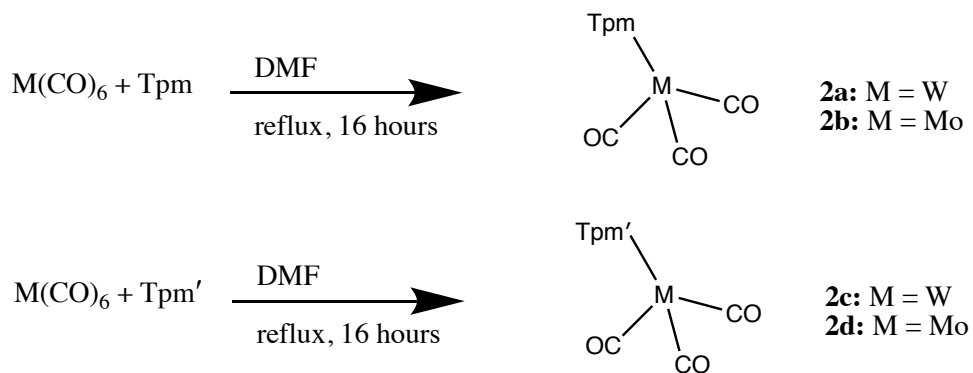
Synthesis of metal complex

The Tpm ligands were synthesized as previously reported with a few minor changes. The ligands are known to be very difficult to synthesize with many reported synthetic routes yielding less than 20 percent yield. The reported reactions with the highest percent yields, had to be rescaled to amounts doable in the laboratory. The scaled back routes resulted in percent yields of 57% for Tpm and 12% for Tpm'. Shown below in **Scheme 1** is the reaction pathway followed in order to synthesize the Tpm, Tpm', and Tpm^{Ph} ligands.



Scheme 1. Synthetic route to Tpm ligands

The Tpm tricarbonyl metal complexes were synthesized as previously reported, with minor changes in the reflux time for the Tpm^{Ph} metal complex (**Scheme 2**). The metal complexes are known to be bright yellow, air sensitive, and highly insoluble in common solvents.



Scheme 2. Synthetic route to neutral Tpm tricarbonyl metal complex

The synthetic routes are not difficult and can be done on multigram scales with yields reaching above 80%. The routes utilized in this work resulted in percent yields between 80 and 90% for

the four various Tpm metal complexes: 90% for TpmW(CO)₃ (**2a**), 90% for TpmMo(CO)₃ (**2b**), 81% for Tpm'W(CO)₃ (**2c**), and 85% for Tpm'Mo(CO)₃ (**2d**).

In previous work done by Dilsky et. al., there were a small sample of cationic seven coordinate Tpm metal complexes that had successfully synthesized and analyzed. These reactions were repeated in the realm of this work with minor deviations from the experimental work of Dilsky. These reactions were previously ran for 2 hours, however it was found within this work that comparable results could be achieved within 30 minutes with all three electrophilic species. It was noted within Dilsky's work that were difficulties working with the cationic molybdenum bromide complexes due to the fluxionality within the complex. This fluxionality arises from the metal complexes desire to be in the most optimal geometry possibly with the seven coordinated ligands, while also maintaining an 18 electron system. Dilsky's previous work, as well as current IR spectra, suggests that there is fluxionality between a 4:3 piano stool geometry and a 3:3:1 geometry, which is evident that both geometries are equally as favorable for the complex. This ultimately leads to difficulties in obtaining NMR data.⁴ Shown below in **Figures 4, 5, and 6** are the three various reactions for the synthesis of the hydride, bromide, and iodide cationic species.

Specifically, TpmM(CO)₃ (**2a-2d**) will undergo reaction with HBF₄ to yield the cationic hydride complex. The hydride complexes have been synthesized for the tungsten and molybdenum complexes of Tpm and Tpm', and for tungsten only with Tpm^{Me}. For [TpmW(CO)₃H]⁺, the hydride ligands are observed at approximately -2.5 ppm with tungsten coupling of approximately 10 Hz.

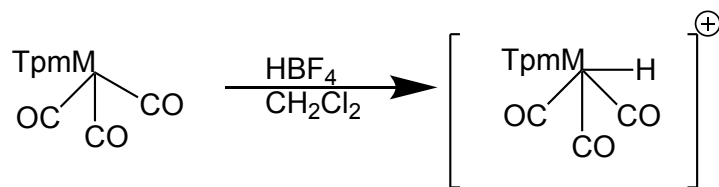


Figure 4. Synthetic route for cationic hydride Tpm metal complexes.

$\text{TpmM}(\text{CO})_3$ will undergo reaction with Br_2 to produce the cationic bromide complex. While all of the complexes exhibit fluxional behaviors between a 3-4 and 3-3-1 geometry, the molybdenum Tpm and Tpm' bromide complexes are extremely fluxional on the NMR time scale at room temperature, resulting in broad ^{13}C NMR signals for the carbon of the CO ligand.⁴

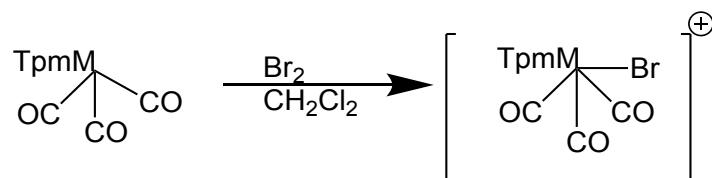


Figure 5. Synthetic route for cationic bromide Tpm metal complexes.

$\text{TpmM}(\text{CO})_3$ will successfully undergo reaction with I_2 to produce the cationic iodide complex. This similarly synthesized iodide derivative is the most stable for both of the metals and all ligands utilized.

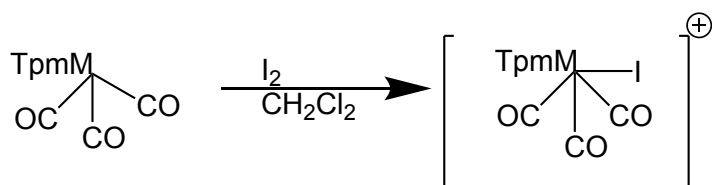


Figure 6. Synthetic route for cationic iodide Tpm metal complexes.

Among these three various cationic complexes, it is seen that when the Tpm ligand and the metal center stay constant, the FTIR stretching frequencies of the CO groups will increase in wave number value as the electronegativity of the newly coordinated cationic ligand increases. When one cationic complex is compared to the precursor neutral six-coordinate complex, it is also seen that the introduction of an electronegative ligand will also increase the FTIR stretching frequencies in regards to the neutral six-coordinate Tpm metal complex.

Tungsten vs. molybdenum metal center:

The amount of electron density present on the metal center can be seen in back bonding trends across the synthesized complexes. In a comparison of tungsten and molybdenum, tungsten has more electron density than molybdenum. This is due to the fact that tungsten is one row lower on the periodic table than molybdenum, meaning that tungsten has a higher overall amount of electrons than molybdenum. The CO groups of the molybdenum metal complex should appear at a higher wave number in the IR spectra than the tungsten metal complex, since there is less electron density available for the π^* CO orbitals in the molybdenum complexes. The specific species which will be compared are TpmW and TpmMo species, Tpm'W and Tpm'Mo species, and the Tpm^{Ph}W and Tpm^{Ph}Mo tricarbonyl species. Solid state IR spectra were obtained for a series of octahedral Tpm, Group 6, tricarbonyl complexes. The data is shown below in **Table 1**.

	TpmM(CO) ₃	Tpm'M(CO) ₃	Tpm ^{Ph} M(CO) ₃
W	1880 and 1743 cm ⁻¹	1888 and 1750 cm ⁻¹	1884 and 1749 cm ⁻¹
Mo	1882 and 1763 cm ⁻¹	1900 and 1764 cm ⁻¹	1891 and 1759 cm ⁻¹

Table 1: Solid state IR stretching frequencies for neutral Tpm metal complexes.

Among the two Tpm metal complexes, the TpmMo(CO)₃ CO stretches appear at 1882 and 1763 cm⁻¹, and in TpmW(CO)₃, the CO stretches appear at 1880 and 1743 cm⁻¹. Among the two Tpm' metal complexes, the Tpm'Mo(CO)₃ CO stretches appear at 1900 and 1762 cm⁻¹, and in Tpm'W(CO)₃, the CO stretches appear at 1888 and 1750. Among the two Tpm^{Ph} metal complexes, the Tpm^{Ph}Mo(CO)₃ CO stretches appear at 1891 and 1759 cm⁻¹, and in Tpm^{Ph}W(CO)₃, the CO stretches appear at 1884 and 1749 cm⁻¹. Since tungsten is one row down from molybdenum, tungsten inherently possesses more electron density, and pushes more electron density into the π* orbitals of the CO ligands, so the CO stretching frequencies are observed at a lower wave number for all tungsten complexes regardless of which Tpm ligand was used.

Tpm, Tpm', Tpm^{Me}, and Tpm^{Ph} ligand: Back bonding trends that are attributed to the varied Tpm ligands can be seen among the complexes. Between the various Tpm ligands, the Tpm' ligand provides the most electron density since it is disubstituted, and the Tpm ligand provides the least electron density. The methyl groups belonging to the Tpm' ligand are electron donating, providing more electron density to the metal center. Tpm' is known to have the capability to provide more electron density to the metal center than the Tpm ligand due to the presence of the methyl groups.⁵ The CO groups of the Tpm' metal complex should appear at the lower wave numbers, and the CO groups of the Tpm metal complex should appear at the highest wave numbers. It is seen that among all four of the varied ligands, there is are nearly identical CO stretching frequencies in the solid state IR. What this means is that in solid state, the Tpm ligand is not impacting the degree of back bonding.

Neutral vs. Cationic tricarbonyl complexes: The CO stretching frequencies were obtained in solid state for a series of neutral Tpm, Group 6, tricarbonyl complexes and in solution for a series of cationic Tpm, Group 6, tricarbonyl complexes. Between both the neutral complex and the cationic complex, there is an increase in the attraction of electrons away from the metal center as a newly coordinated cationic ligand is introduced to the neutral metal complex. As the electronegative ligand is introduced, there is less available electron density present in the metal center to participate in back bonding, which will result in an overall higher wave number present in the IR. Therefore, it should follow that the CO groups of the cationic tricarbonyl complex will have a higher stretching frequency than that of the neutral tricarbonyl complex. Shown below in **Table 2** are both the neutral and cationic tricarbonyl molybdenum and tungsten metal complexes.

	TpmM(CO) ₃	[TpmM(CO) ₃ H] ⁺ BF ₄ ⁻
W	1880 and 1743 cm ⁻¹	2022, 1935, 1912
Mo	1882 and 1763 cm ⁻¹	2029, 1939, 1921.

Table 2. Solid state and solution IR stretching frequencies for neutral and cationic Tpm species

As seen in **Table 2**, the CO stretching frequencies for the neutral tungsten and molybdenum complexes have a lower stretching frequency than the cationic complexes. Therefore, as an electronegative ligand is coordinated to a neutral tricarbonyl complex, the CO stretching frequency of the new cationic complex will be higher than that of the neutral complex.

H vs. Br vs. I ligand: The CO stretching frequencies for a series of cationic Tpm, Group 6, tricarbonyl complexes were obtained in solution. Between the three ligands, the bromo ligand has the highest electronegativity, the iodo the next, and the hydrido the lowest electronegativity. Electronegativity is a measure of the willingness of an atom to attract electrons in a covalent bond. The electron density is attracted towards the more electronegative ligand, such as the I or Br. These compounds have a higher electronegativity in comparison to the metal center, which means there is less electron density present on the metal center. The results from this interaction are a higher wave number in the IR. Therefore, the CO groups of the bromo transition metal complex will have the highest stretching frequency, the CO groups of the iodo transition metal complex will have the next highest, and the CO groups of the hydrido transition metal complex will have the lowest stretching frequency. **Table 3** organizes the twelve various transition metal complexes into both columns based on the metal center, and rows based on the increasing electronegativity of the anionic ligand.

	$[\text{TpmM}(\text{CO})_3\text{H}]^+\text{BF}_4^-$	$[\text{TpmM}(\text{CO})_3\text{I}]^+\text{I}^-$	$[\text{TpmM}(\text{CO})_3\text{Br}]^+\text{Br}^-$
W	2022, 1935, 1912	2036, 1960, 1928	2045, 1966, 1925
Mo	2029, 1939, 1921	2044, 1976, 1945	2056, 1989, 1946
	$[\text{Tpm}'\text{M}(\text{CO})_3\text{H}]^+\text{BF}_4^-$	$[\text{Tpm}'\text{M}(\text{CO})_3\text{I}]^+\text{I}^-$	$[\text{Tpm}'\text{M}(\text{CO})_3\text{Br}]^+\text{Br}^-$
W	2012, 1927, 1893	2054, 2032, 1931	2036, 1958, 1928
Mo	2020, 1938, 1918	2043, 2019, 1956	2048, 1973, 1952

Table 3: Solution IR stretching frequencies for Tpm group six cationic species

In **Table 3**, the CO stretching frequencies for the tungsten and molybdenum Tpm complexes with hydrido, iodo, and bromide ligands are shown. For $[\text{TpmW}(\text{CO})_3\text{H}][\text{BF}_4]$, the CO stretching frequencies are observed at 2022, 1935, and 1912 cm^{-1} , for $[\text{TpmW}(\text{CO})_3\text{I}][\text{I}]$, the CO stretching

frequencies are observed at 2036, 1960, and 1928 cm^{-1} , and in $[\text{TpmW}(\text{CO})_3\text{Br}][\text{Br}]$, the CO stretching frequencies are observed at 2045, 1966, and 1925 cm^{-1} . For all four series, it is evident that the bromo complex has the highest CO stretching frequencies. The CO stretching frequencies for the iodo complex are observed at lower wave numbers, and the CO stretching frequencies for the hydrido complex are observed at the absolute lowest wave numbers. Among the three ligands, the electronegativity of these ligands decreases from bromine, to iodine, to hydrogen. It is observed that the complex with the highest CO stretching frequencies also has the most electronegative ligand. Therefore, it is shown that by increasing or decreasing the electronegativity of coordinated ligands, the CO stretching frequencies observed from the complex will increase or decrease as well, respectively.

For $[\text{TpmMo}(\text{CO})_3\text{H}][\text{BF}_4]$, the CO stretching frequencies are observed at 2029, 1939, and 1921 cm^{-1} , for $[\text{TpmMo}(\text{CO})_3\text{I}][\text{I}]$, the CO stretching frequencies are observed at 2044, 1976, and 1945 cm^{-1} , and in $[\text{TpmMo}(\text{CO})_3\text{Br}][\text{Br}]$, the CO stretching frequencies are observed at 2056, 1989, and 1946 cm^{-1} . These Tpm molybdenum complexes follow similar trends as seen with the Tpm tungsten complexes. For the molybdenum series, it is seen that the bromo complex has the highest CO stretching frequencies, the iodo complex has CO stretching frequencies at lower wave numbers, and the hydrido complex has CO stretching frequencies observed at the lowest wave numbers.

For $[\text{Tpm}'\text{W}(\text{CO})_3\text{H}][\text{BF}_4]$, the CO stretching frequencies are observed at 2012, 1927, and 1893 cm^{-1} , for $[\text{Tpm}'\text{W}(\text{CO})_3\text{I}][\text{I}]$ the CO stretching frequencies are observed at 2054, 2032, and 1931 cm^{-1} , and in $[\text{Tpm}'\text{W}(\text{CO})_3\text{Br}][\text{Br}]$ the CO stretching frequencies are observed at 2036, 1958, and 1928 cm^{-1} . The trends seen in the Tpm' tungsten series follow those which were observed for both the Tpm tungsten and Tpm molybdenum series.

For [Tpm'Mo(CO)₃H][BF₄], the CO stretching frequencies are observed at 2020, 1938, and 1918 cm⁻¹, for [Tpm'Mo(CO)₃I][I] the CO stretching frequencies are observed at 2043, 2019, and 1956 cm⁻¹, and in [Tpm'Mo(CO)₃Br][Br] the CO stretching frequencies are observed at 2048, 1973, and 1952 cm⁻¹.

NMR Analysis of Tpm metal complexes: The ¹H NMR signals for the series of Tpm, Group 6, tricarbonyl complexes were obtained in CD₂Cl₂ relative to a TMS standard. For each of the complexes, whether neutral or cationic, the pyrazole rings of the Tpm ligands in the ¹H NMR are detected as equivalent, as is observed similarly for the closely related Tp and Tp' species.⁴ Among both neutral and cationic complexes, the chemical shifts for the hydrogens in the 4 position of the pyrazole rings are observed anywhere from 5 ppm to 6.5 ppm. The hydrogens in the 3 or 5 positions of the pyrazole rings, if present, are observed anywhere from 8 ppm to 9 ppm, and the hydrogens of the methyl groups on the Tpm' and Tpm^{Me} pyrazole rings are observed anywhere from 2 ppm to 3 ppm. The ¹H NMR signals for all of the hydrogens except for the central hydrogen had minimal variability, resulting in conclusive evidence that these hydrogens were negligibly affected by changes in the metal center, Tpm analog, or charge of the metal complex.

However, it was observed that the central tetrahedral hydrogen exhibited very unusual patterns in the ¹H NMR spectra. Among the cationic hydrido, bromo, and iodo derivatives of TpmM(CO)₃ complexes, the central tetrahedral hydrogen exhibited extremely large chemical shift differences among all three complexes.⁶ It was noted that the more electronegative the ligand, the greater the downfield shift of the hydrogen on this carbon. In previous works, the

complex of interest utilized the Tp ligand, and the hydrogen of interest was on a boron instead of a carbon and was therefore unobservable in the ^1H NMR, allowing for no comparable trends to be seen. These experiments, therefore, were focused on whether the large chemical shift differences observed by Dilsky for the central hydrogen on the original Tpm metal complexes would also be seen for Tpm metal complexes utilizing other Tpm analogues, such as Tpm' and Tpm^{Me}. The central hydrogen was indeed observed to exhibit the same significant chemical shift differences reported by Dilsky for the bromide, iodide, and hydride derivatives for the Tpm complex. (Table 4).

	$[\text{TpmM}(\text{CO})_3\text{Br}]^+$	$[\text{TpmM}(\text{CO})_3\text{I}]^+$	$[\text{TpmM}(\text{CO})_3\text{H}]^+$
W	13.1 ppm	11.4 ppm	9.56 ppm
Mo	12.8 ppm	11.9 ppm	9.54 ppm
	$[\text{Tpm}'\text{M}(\text{CO})_3\text{Br}]^+$	$[\text{Tpm}'\text{M}(\text{CO})_3\text{I}]^+$	$[\text{Tpm}'\text{M}(\text{CO})_3\text{H}]^+$
W	8.03 ppm	7.99 ppm	8.09 ppm
Mo	8.16 ppm	8.14 ppm	8.03 ppm
	$[\text{Tpm}^{\text{Me}}\text{M}(\text{CO})_3\text{Br}]^+$	$[\text{Tpm}^{\text{Me}}\text{M}(\text{CO})_3\text{I}]^+$	$[\text{Tpm}^{\text{Me}}\text{M}(\text{CO})_3\text{H}]^+$
W	Not Synthesized	8.67 ppm	8.26 ppm

Table 4: ^1H NMR (CD_2Cl_2) chemical shift values for bromide, iodide, and hydride derivatives of varying Tpm tungsten and molybdenum complexes.

Although there were significant chemical shift differences obtained for the central hydrogen of the Tpm metal complexes, substantial differences were not seen for the Tpm' or the two Tpm^{Me} complexes synthesized. The downfield chemical shift of the hydrogen for the central

hydrogen of the Tpm' complex was consistent for all three cationic species, with the NMR signal ranging from 7.9 ppm to 8.1 ppm. For the Tpm^{Me} complexes, the NMR signal was seen to shift from 7.8 for the neutral species, to 8.3 for the hydride species, and to 8.7 for the iodide species. The changes in chemical shifts for the Tpm^{Me} complexes were observed to not be as drastic as previously seen with the Tpm metal complexes. However, there was a much more significant difference in the chemical shifts than what was seen for the Tpm' metal complexes, which was informative that the total electron density of the metal complex might be contributing to the change in the NMR signal for the central hydrogen. It has been documented that for pyrazolylborate ligands, Tp' is a much more electron rich ligand than Tp. While the Tpm ligands have not been as extensively studied, through the CO stretching frequencies, it is known that Tpm' is an overall more electron rich ligand than Tpm. In the far less electron rich Tpm complexes, when an electronegative substituent is present on the metal, enough electron density is pulled from the Tpm ligand to impact the electronic environment of the central hydrogen. Since both the Tpm' and Tpm^{Me} ligands are more electron rich than the Tpm counterpart, the same impact on the central hydrogen is not observed as evidenced from the NMR.

Conclusion

Throughout this work with the Tpm and Tpm derivative metal complexes, it was found that both the electronegativity of the newly coordinated anionic ligand as well as the total electron density of the transition metal complex were the largest factors contributing to the chemical shift effects of the central tetrahedral hydrogen. In the future, more work will be done to further characterize more Tpm derivative metal complexes, such as the Tpm^{Ph} and Tpm^{Me}

metal complexes. Also, more Tpm derivatives will be synthesized, such as a Tpm derivative with an acetyl functional group present.

Acknowledgements

I would like to acknowledge Eli Lilly and Company through the Lilly Undergraduate Research Grant for providing the funding necessary for me to perform my research, and I would also like to thank Butler University for providing the laboratory equipment necessary to perform my research. I would like to thank Cody Carley for providing me with many of my starting ligands that were vital to my research. Lastly, I would like to give an enormous thank you to Dr. Stacy O'Reilly, for not only being one of the most influential mentors throughout my time performing research at Butler University, but also for allowing me to grow into the scientist I am today that will continually push the boundaries of my knowledge into unexplored areas for many years into the future.

References

1. Ashby, J.; Elliott, B. M. Toxicity of Heterocycles *Chemistry, Molecular Sciences and Chemical Engineering* **1984**, *1*, 111-141.
2. Trofimenko, S. Geminal Poly(1-pyrazolyl)alkanes and their coordination chemistry. *Journal of the American Chemical Society* **1970**, *92* (17), 5118–5126.

3. Goodman, M. A.; Nazarenko, A. Y.; Casavant, B. J.; Li, Z.; Brennessel, W. W.; Demarco, M. J.; Long, G.; Goodman, M. S. Tris(5-methylpyrazolyl)methane: Synthesis and Properties of Its Iron(II) Complex. *Inorganic Chemistry* **2011**, *51* (2), 1084–1093.
4. Feng, S. G.; Gamble, A. S.; Philipp, C. C.; White, P. S.; Templeton, J. L. Synthesis and Characterization of Chiral (Hydridotris(3,5-dimethylpyrazolyl)borato)tungsten(II) Alkyne Complexes. *Organometallics* **1991**, *10* (10), 3504–3512.
5. Reger, D.; Grattan, T.; Brown, K.; Little, C.; Lamba, J.; Rheingold, A.; Sommer, R. Syntheses Of Tris(Pyrazolyl)Methane Ligands And {[Tris(Pyrazolyl)Methane]Mn(CO)₃}SO₃CF₃ Complexes: Comparison Of Ligand Donor Properties. *Journal of Organometallic Chemistry* **2000**, *607*, 120-128.
6. Dilsky, S. Molybdenum And Tungsten Complexes Of The Neutral Tripod Ligands HC(Pz)₃ And Mec(Ch₂pPh₂)₃. *Journal of Organometallic Chemistry* **2007**, *692*, 2887-2896.